Atmos. Chem. Phys. Discuss., https://doi.org/10.5194/acp-2018-721
Manuscript under review for journal Atmos. Chem. Phys.
Discussion started: 4 September 2018

Atmospheric Chemistry and Physics Discussions

Diagnosis of dust- and haze pollution-impacted PM_{10}, $PM_{2.5}$, and PM_1 aerosols observed at Gosan Climate Observatory

Xiaona Shang[1], Meehye Lee[1*], Saehee Lim[1], Örjan Gustafsson[2]
Gangwoong Lee[3], Limseok Chang[4]

[1] Department of Earth & Environmental Sciences, Korea University, Seoul, South Korea

[2] Department of Applied Environmental Science (ITM) and the Bolin Centre for Climate Research, Stockholm University, 10691 Stockholm, Sweden

[3] Department of Environmental Science, Hankuk University of Foreign Studies, Seoul, South Korea

[4] National Institute of Environmental Research (NIER), Incheon, South Korea

[*] Correspondence to: M. Lee (meehye@korea.ac.kr)

Atmos. Chem. Phys. Discuss., https://doi.org/10.5194/acp-2018-721
Manuscript under review for journal Atmos. Chem. Phys.
Discussion started: 4 September 2018

Atmospheric Chemistry and Physics Discussions

Abstract

In East Asia, soil dust is a major component of aerosols and is mixed with various pollutants during transport, resulting in large uncertainty in climate and environmental impact assessment and relevant policymaking. To diagnose the influence of soil dust and anthropogenic pollution on bulk aerosol, we conducted long-term measurements of mass, water-soluble ions, and carbonaceous compounds of PM_{10}, $PM_{2.5}$, and PM_1 at Gosan Climate Observatory, South Korea, from August 2007 to February 2012. The principle component analyses of all measured species reveal that the impact of anthropogenic pollution, soil dust, and agricultural fertilizer accounts for 46%, 16%, and 9% of the total variance, respectively. Particularly, the loadings of agricultural component were high in the warmer months with the least occurrence of high concentration events and have increased over time. In mode analysis of PM_{10}, $PM_{2.5}$, and PM_1 mass concentrations, the mean + σ was comparable to the 90^{th} percentile and thus, suggested as a robust criterion that determines the substantial impact of soil dust and haze pollution on particulate matter. The results of this study imply that non-combustion sources such as soil dust will impose constraints to the reduction of $PM_{2.5}$ as well as PM_{10} concentrations. In addition, questions are raised as to whether the yearly average concentration is suitable for environmental standard in northeast Asian region.

Atmos. Chem. Phys. Discuss., https://doi.org/10.5194/acp-2018-721
Manuscript under review for journal Atmos. Chem. Phys.
Discussion started: 4 September 2018

Introduction

Dust particles are dominant atmospheric aerosols and account for more than 60% of the total global dry aerosol mass burden (Textor et al., 2006). The emission of dust ranges from 1000 to 3000 Tg yr^{-1} (Zender et al., 2004). Dust particles are abundant in coarse mode, which is represented by PM_{10}. Recently, a new type of dust particle has been observed in submicron size that was long-range transported from dry lake deposits in northern China. These particles are more abundant in salts and mineral constituents compared with typical soil dust (Shang et al., 2018). The high-mass loading of dust adversely affects air quality and causes climate change. In regional to global earth's environment, mineral dust contributes to a radiative forcing of $-0.3 \sim +0.1$ W m^{-2} with a large uncertainty (IPCC, 2007, 2013) because emission source, chemical and mineralogical composition, and particle size vary in a wide range (Choobari et al., 2014). Dust particles have also been predicted to reduce the rate of ozone production (Dickerson et al., 1997) and promote new particle formation and growth by mixing with other pollutants (Nie et al., 2014; He et al., 2014). Their role in climate change is further highlighted by modifying cloud microphysical process via cloud droplet activation (Bègue et al., 2015) and CO_2 uptake via ocean fertilization (Pabortsava, et al., 2017).

A large amount of dust is found over arid regions in North Africa, North China and South Mongolia (Choobari et al., 2014). In East Asian desert areas, soil type significantly varies from arid and semi-arid deserts to loess deposits and dry lake deposits, depending on the formation process and climate (Zhang et al., 2009). Dust particles generated from these regions are different in chemical and mineralogical composition (Cheng et al., 2012; Kunwar and Kawamura, 2014; Liu et al., 2011; Tao et al., 2014; Su and Toon, 2011), leading to different environmental effects. For example, African dust contains more iron oxides mineral in the form of hematite as compared with those from Asia (Formenti et al., 2011; 2014), implying greater light absorption (Zhang et al., 2015). Among atmospheric aerosols generated from variety of emissions (Geng et al., 2014). EC is a main species absorbing light and measured as black carbon (BC) (Han et al., 2010; Saleh et al., 2014). In Northeast Asia, aerosols from various sources are often mixed together while being transported (Kim et al.,

2007) and dust plumes have been identified as enhanced concentrations of sulfate, nitrate, ammonium, OC or EC over the Korean peninsula (Shin et al., 2015).

An array of AERONET and satellite observations is a vital tool for investigating atmospheric aerosol at regional and global scales (Zhuang et al., 1992; Zhang et al., 2003; Jin et al., 2016; Nazari et al., 2016). Because these techniques measure the extinction of bulk aerosols, it is crucial to accurately estimate the optical property of major aerosol constituents (e.g., Kim et al., 2007) in order to assess the anthropogenic contribution to total aerosol burden and its climate effect using remote sensing data. However, it is still a big challenge to estimate the optical property of main aerosol types especially dust particles in East Asia, because their property is not only dependent on source regions (Huang et al., 2014) but also modified during transport through aging and mixing with pollutants (McFarlane et al., 1992; Von Salzen et al., 2005; Bäumer et al., 2007; Kim et al., 2011). For instance, the mixture of dust and pollutant caused a significant increase of radiative forcing by 0.06 Wm^{-2} (Zhang et al., 2013a; Mishra et al., 2010; Li et al., 2012). In this context, it is important to figure out the extent of dust particles in the atmosphere and distinguish them from bulk aerosol particles. For instance, the ratio of $PM_{10}/PM_{2.5}$ has been employed to eliminate the effect of soil dust from $PM_{2.5}$ when determining the mass absorption coefficient of OC (Chung et al., 2012).

In this study, to diagnose the impact of airborne dust and anthropogenic pollution on atmospheric particulate matter and find out feasible criteria, the five-year measurements of mass, water-soluble ions, and carbonaceous compounds for PM_{10}, $PM_{2.5}$, and PM_1 were analyzed using statistical methods. The long-term and composite measurements of particulate matter in different sizes are scarce in the study region. The results of mass mode analysis and principle component analysis will provide insight into the role and significance of mineral dust and haze pollution on particulate matter and further its control strategies in northeast Asia.

Atmos. Chem. Phys. Discuss., https://doi.org/10.5194/acp-2018-721
Manuscript under review for journal Atmos. Chem. Phys.
Discussion started: 4 September 2018

1 Methodology

Aerosol samples were collected separately for PM_1, $PM_{2.5}$, and PM_{10} onto 37 mm Teflon and Quartz filters (Pall, Corp.) using sharp-cut cyclones (URG, USA) at the Gosan Climate Observatory (GCO) from 2007 to 2012. Sampling was undertaken for a period of 24 h from 10:00 to 10:00 the next day. A total of 152 sets of samples were collected and analyzed for water-soluble inorganic ions and carbonaceous compounds. Details about the measurement methodology can be found in Lim et al. (2012, 2014). During the five-year period, five dust and eleven haze events were recorded across Korea by the Korea Meteorological Administration (KMA) mostly during the cold seasons from late fall to spring (Fig. 1).

Teflon filters were conditioned for 24 h in desiccators (SANPLATEC, Japan) under a relative humidity of approximately 30%–40% and weighed before and after sampling using an analytical balance (Denver, Germany). Water-soluble species were extracted from the filters into a solution comprising a mixture of 19 mL distilled water and 1 mL methanol. Water-soluble ions, including Cl^-, NO_3^-, SO_4^{2-}, Na^+, NH_4^+, K^+, Mg^{2+}, and Ca^{2+} were analyzed via ion chromatography (IC 25, Dionex, USA). For this analysis, 500 μL of sample was injected by an auto-sampler into the AG11 and AS11 columns for anions or CG11 and CS11 columns for cations (Dionex, USA). The eluent and suppressor were 39 mM KOH and ASRSIIULTRA-4 mm and 20 mM MSA and CSRSIIULTRA-4 mm for anions and cations, respectively. Finally, concentrations were determined using a conductivity detector (Dionex, USA), which was calibrated against eight aqueous standards. The detection limit, defined as 3σ, was approximately 0.01–0.09 $\mu g/m^3$.

Carbonaceous components were measured at the Desert Research Institute (the thermal/optical reflectance (TOR) method, Reno, NV, USA) using the Interagency Monitoring of Protected Visual Environments (IMPROVE) TOR protocol. OC comprising OC1, OC2, OC3, and OC4 was determined at 120ºC, 250ºC, 450ºC, and 550ºC, respectively, in a He atmosphere. EC was analyzed as EC1, EC2, and EC3 at 550ºC, 700ºC, and 850ºC, respectively, after introducing 2% O_2/ 98% He. Pyrolyzed OC (OP) was measured in the

O_2/He atmosphere before the reflected light returned to its initial value (Lim et al., 2012; 2014).

2 Measurement overview

From August 2007 to December 2012, the average PM_{10}, $PM_{2.5}$, and PM_1 mass concentrations of all measurements were 30 μg/m^3, 19 μg/m^3, and 14 μg/m^3, respectively (Table 1). The PM_{10} mass was almost equally partitioned between <1 μm and 1 – 10 μm. Moreover, the mass of particles between 1 μm and 2.5 μm was considerable and comprises 26% of $PM_{2.5}$ mass. As summarized in Table 1, SO_4^{2-} and OC were the most abundant, followed by NH_4^+ and NO_3^-. These four species accounted for 48%, 58%, and 69% of the PM_{10}, $PM_{2.5}$, and PM_1 mass, respectively. Of these species, SO_4^{2-}, NH_4^+, and EC were pre-dominant in PM_1, which corresponds to more than 75% of those in PM_{10}. In comparison, about 65% of OC was partitioned into PM_1. It was even less for NO_3^- as 33%. It is well known that NO_3^- is more abundant in coarse mode particles due to high affinity to soil mineral. It is also noteworthy that a substantial amount of OC and EC (20 %) was associated with particles between 1 μm and 2.5 μm. Of OC sub-components, OC3 and OC4 were mainly associated with coarse particles. It is evident that Na^+ and Cl^- were highly enriched in coarse particles between 2.5 μm and 10 μm.

The high PM_{10} mass was usually observed in the spring along with increased concentrations of Ca^{2+} and Mg^{2+} (Fig. 1). In comparison, the mass of PM_1 was higher in the cold season (fall to winter) when the concentrations of SO_4^{2-}, NO_3^-, NH_4^+, K^+, OC, and EC were highly elevated. High $PM_{2.5}$ concentrations were observed in both winter and spring periods. Overall, the three particle masses and their major constituents were highly elevated when dust and haze events occurred.

Atmos. Chem. Phys. Discuss., https://doi.org/10.5194/acp-2018-721
Manuscript under review for journal Atmos. Chem. Phys.
Discussion started: 4 September 2018

Five dust events took place in March, May, November, and December for the entire experiment period. Upon dust incidence, the daily average mass concentrations of PM_{10} and $PM_{2.5}$ were enhanced by 3 and 2 times, respectively. In comparison, concentrations of mass, secondary ions, and carbonaceous compounds were elevated more than two times in PM_1 during the haze events from October to April. On March 20, 2010, dust and haze event occurred concurrently, leading to a maximum PM_{10} concentration of 199 $\mu g/m^3$. PM_{10} concentrations were occasionally elevated without an official report of KMA on dust occurrence. For instance, in March 2008, the concentrations of PM_{10} mass, Ca^{2+}, and Mg^{2+} were higher than those of dust event days.

3 PCA analysis of PM_{10}, $PM_{2.5}$, and PM_1

Principle component analysis (PCA) was conducted for all measured species of PM_{10}, $PM_{2.5}$, and PM_1 aerosols including water-soluble ions, OC, EC, and mass for the whole period. PCA analysis identifies the correlation of variables through orthogonal transformation and summarizes the main characteristics of measurement data set. In PCA analysis, two components are usually selected. In this study, the principle component 1 and 2 accounted for more than 60% of the total variance of PM_{10}, $PM_{2.5}$, and PM_1. The principle component 1 (PC1) was composed of high loadings for SO_4^{2-}, NO_3^-, NH_4^+, K^+, OC, and EC, especially in PM_1 (Fig. 2). These six species contributed almost equally to the PC1, which explained 46% of the total variance. In contrast, the principle component 2 (PC2) explained 16% of the total variance and was characterized by high loadings for Na^+, Cl^-, Mg^{2+} and Ca^{2+}, mainly in PM_{10} and $PM_{2.5}$. Interestingly, the principle component 3 (PC3) comprising 9% of the total variance, was associated with high loadings for NH_4^+ and Ca^{2+}, particularly in PM_{10} (Fig. 2 and 3). These three independent factors explain more than 70% of the total variance.

As the most abundant species, SO_4^{2-} and NO_3^- concentrations were highly correlated with PC1 loadings for all three-size particles (Fig. 3), confirming that the PC1 represents the influence of anthropogenic pollution sources (Zhang et al., 2013b). So were OC2 and EC1

that have been reported to originate from biomass combustion sources (e.g., Lim et al., 2012). In PC2, the loadings for Ca^{2+}, Mg^{2+}, Na^{+}, and Cl^{-} were the highest and well correlated with OC4 concentration in $PM_{2.5}$ and PM_{10}, which used to be elevated upon dust events (Lim et al., 2012). In saline dust, the concentrations of Ca^{2+}, Na^{+}, and Cl^{-} were enhanced concurrently with OC sub-component (Zhang et al., 2014; Shang et al., 2018; O'Dowd et al., 2004; Griffith et al., 2010). The sea-salt contribution of Ca^{2+} was estimated to be 12% in $PM_{2.5}$ and 19% in PM_{10}, assuming that sodium was derived solely from sea salt. In this study, the measurements of water-soluble ions demonstrate that the contribution of sea salt species was found to reach the maximum in summer when aerosol loading is at its minimum under influence of marine air. Thus, the PC2 represents the impact of dust particles including alkaline soils. NH_4^{+} concentration was moderately related to PC3 loadings in $PM_{2.5}$ and PM_{10}. In particular, a relatively good correlation of NH_4^{+} with Ca^{2+} in PM_{10} indicates the agricultural influence due to fertilizer use. It is noteworthy that PC3 loading was high in spring and summer when the concentrations of particulate matter were low with reduced continental outflows. In addition, the PC3 loadings increased with time, reaching to the highest in 2010. The recent studies also reported that in China, NH_3 emission was increased due to fertilizer application and NH_4^{+} concentration was higher in spring and summer than the other seasons (Warner et al, 2017; Kang et al., 2016).

Therefore, the three principle components manifest the main sources of particulate matters in the study region. As anthropogenic sources, PC1 is predominant in PM_1 and $PM_{2.5}$. PC2 demonstrates the influence of soil dust on PM_{10} and $PM_{2.5}$. Fertilizer use is likely responsible for the variance of PC3. In order to estimate the contribution of these three factors to the mass of PM_{10}, $PM_{2.5}$, and PM_1 at GCO, multi-linear regression analysis was conducted using factor loadings, of which result is given below:

$$PM_{10}\ (\mu g/m^3) = 31.1 + 4.7\,PC1 + 3.7\,PC2 + 4.1\,PC3 \quad (r = 0.89, P = 0.03) \quad (1)$$

$$PM_{2.5}\ (\mu g/m^3) = 19.2 + 3.1\,PC1 + 0.4\,PC2 + 1.9\,PC3 \quad (r = 0.95, P = 0.03) \quad (2)$$

$$PM_{1}\ (\mu g/m^3) = 14.8 + 2.5\,PC1 - 0.7\,PC2 + 1.6\,PC3 \quad (r = 0.93, P = 0.04) \quad (3)$$

, where PC1, PC2, and PC3 are factor loadings.

220

221 The intercepts of these three equations are equivalent to the average concentrations for PM_{10},
222 $PM_{2.5}$, and PM_1 (Table 1 and 2). It confirms that the three PCs are sufficient enough to
223 explain the variation of aerosol masses observed at GCO. It is evident that PC1 is a dominant
224 factor determining the particulate mass of PM_{10} (63%) as well as PM_1 (99%) and $PM_{2.5}$ (90%).
225 PC2 was most evident in PM_{10} (36%) and not negligible in $PM_{2.5}$ (9%). It is worthy
226 emphasizing that NH_4^+ factor was distinguished as PC3, even though its contribution was the
227 least. In addition, the very small or negative loading of PC2 for $PM_{2.5}$ and PM_1 suggests the
228 scavenging of anthropogenic pollutants on dust particles.

229

230 **4 Diagnosis of dust and haze**

231

232 While soil dust has been recognized as a main driver for high PM_{10} mass in northeast Asia
233 (Yang et al., 2009), air pollution events are typically distinguished by the concentrations of
234 $PM_{2.5}$ (EPA, 2012). In Korea, the aerosol mass concentrations have been often elevated upon
235 Asian dust or haze occurrence. In this context, mode analysis of PM_{10}, $PM_{2.5}$, and PM_1 mass
236 concentrations was conducted to diagnose the impact of dust and haze particles on particulate
237 matter. The frequency distributions of all PM_{10}, $PM_{2.5}$, and PM_1 measurements are shown in
238 Figure 4. For the three-size aerosol masses, the main-mode concentrations are comparable to
239 the median concentrations (Table 3 and Fig. 4). The main-mode concentration of PM_{10} and
240 $PM_{2.5}$ was 25 $\mu g/m^3$ and 16 $\mu g/m^3$, respectively, which are much lower than those of national
241 standard of annual mean of 50 $\mu g/m^3$ and 25 $\mu g/m^3$, respectively. The main-mode
242 concentration of PM_1 (11 $\mu g/m^3$) was similar to the air quality guideline of the World Health
243 Organization (WHO) for $PM_{2.5}$ (10 $\mu g/m^3$) (WHO, 2006). Of $PM_{2.5}$ mass, the contribution of
244 mineral dust was estimated to be ~10% in previous section, which is equivalent to about 2
245 $\mu g/m^3$.

246

247 The mean concentrations of the three types of particulate matters were higher than their
248 median and main-mode concentrations and the standard deviations were comparable to the
249 median concentrations. These results show that mass concentrations varied in a wide range

due to high concentration events. For PM_{10}, the mean+σ of 52 μg/m^3 was close to the national standard of PM_{10} annual average concentration. While the mean+σ concentration of $PM_{2.5}$ was higher by 28% than the national standard of 25 μg/m^3, the mean+σ of PM_1 (25 μg/m^3) met the annual standard of $PM_{2.5}$ concentration. The mean+σ concentrations of PM_{10}, $PM_{2.5}$, and PM_1 were commensurate with the 90th percentiles that generally represent the highest concentration of the long-tern measurements.

In Korea, dust occurrence is determined by eye observation and haze is recorded when RH is less than 75 % and visibility is between 1 km and 10 km. The concentrations of individual dust and haze samples are presented in the bottom of Figure 4. While the PM_{10} and $PM_{2.5}$ concentrations of five dust events are placed in the range above the mean+σ, all of the high PM_{10} concentrations were not observed on dust days. In contrast, the concentrations of all haze samples were over the mean+σ of PM_1 (Fig. 4).

When PM_{10} and $PM_{2.5}$ mass belong to the top 10%, their Ca^{2+} and Mg^{2+} concentrations were also within the highest 10 % of the entire measurements. Particularly, Ca^{2+} concentration (0.7 μg/m^3) was 3 times as high as the average concentration for both PM_{10} and $PM_{2.5}$ (Table 1), implying that dust effect is not negligible in $PM_{2.5}$.

At GCO, the five-year measurements of aerosol mass and chemical composition reveal that the top 10 % of PM_{10}, $PM_{2.5}$, and PM_1 mass was affected by dust or haze plumes and their effect is traceable by the 90th percentile mass concentrations of particulate matter. If PM_{10} or $PM_{2.5}$ mass concentrations are above the 90th percentile, airborne dust particles played a substantial role in mass enhancement, regardless of the occurrence of event. Likewise, anthropogenic pollution is a main driver for enhanced PM_1 and $PM_{2.5}$ mass concentrations if their concentrations are greater than the 90th percentile. For $PM_{2.5}$, the impact of mineral dust should be considered in northeast Asia region downwind of the dust belt.

Atmos. Chem. Phys. Discuss., https://doi.org/10.5194/acp-2018-721
Manuscript under review for journal Atmos. Chem. Phys.
Discussion started: 4 September 2018

Atmospheric Chemistry and Physics Discussions

5 Conclusions

At GCO, filter samples for PM_1, $PM_{2.5}$, and PM_{10} were collected and their mass, water-soluble inorganic ions and carbonaceous compounds were analyzed from 2007 to 2012. For the entire period, the average concentrations of PM_{10}, $PM_{2.5}$, and PM_1 were 30, 19, and 14 $\mu g/m^3$, respectively. $PM_{2.5}$ accounted for 63% of PM_{10}, while PM_1 comprised 74% of $PM_{2.5}$ on average.

From the principle component analysis using all measured species for PM_{10}, $PM_{2.5}$, and PM_1, the three principle components (PC1, PC2, and PC3) were distinguished, which explained 46%, 16%, and 9% of the total variances, respectively. The PC1 representing the effect of anthropogenic pollution was characterized by high loadings of SO_4^{2-}, NO_3^-, NH_4^+, K^+, OC, and EC. The PC2 was distinct with high loadings for Ca^{2+} and Mg^{2+} that originate from soil dust. Although the contribution was low, the PC3 was significant for two reasons. First, the loadings of PC3 showed an increasing tendency over time. In addition, the PC3 loadings were discernible during warm season, in contrast to other two components that explain the variations of mass and major constituents of aerosol during cold season. The multiple regression using the three PC loadings shows that the anthropogenic pollution accounted for 99 % and 63 % of PM_1 and PM_{10} mass variation, respectively. The effect of soil dust was the largest on PM_{10} (36%) and not negligible on $PM_{2.5}$ (~10%).

The mode analysis of PM_{10}, $PM_{2.5}$, and PM_1 mass concentrations demonstrates that the main mode was commensurate with the median concentration and the mean + σ was comparable to the concentration of the 90^{th} percentile. It indicates that the average mass concentration is highly susceptible to high-concentration episodes. Consequently, the mean+σ is suggested as a robust criterion that determines the substantial impact of soil dust or pollution plumes on PM_{10}, $PM_{2.5}$, and PM_1. Furthermore, the results of this study reveal that in northeast Asia, non-combustion sources such as soil dust with impose constraints to the reduction of $PM_{2.5}$ as well as PM_{10} concentrations and raise questions about the efficacy of yearly average concentrations as environmental standards.

Acknowledgments

This research was supported by the National Strategic Project-Fine Particle of the National Research Foundation of Korea (NRF) funded by the Ministry of Science and ICT (MSIT), the Ministry of Environment (ME), and the Ministry of Health and Welfare (MOHW) (2017M3D8A1092015). We also thank the Korea Meteorological Administration for supplying event information including dust and haze, the National Institute of Environmental Research, Gwangju Institute of Science and Technology, and Seoul National University for supporting the experimental data.

References

Bäumer, D., Lohmann, U., Lesins, G., Li, J., and Croft, B.: Parameterizing the optical properties of carbonaceous aerosols in the Canadian Centre for Climate Modeling and Analysis Atmospheric General Circulation Model with impacts on global radiation and energy fluxes, J. Geophys. Res. Atmos., 112(D10), https://doi.org/10.1029/2006JD007319, 2007.

Bègue, N., Tulet, P., Pelon, J., Aouizerats, B., Berger, A., and Schwarzenboeck, A.: Aerosol processing and CCN formation of an intense Saharan dust plume during the EUCAARI 2008 campaign, Atmos. Chem. Phys., 15, 3497-3516, https://doi.org/10.5194/acp-15-3497-2015, 2015.

Cheng, M. C., You, C. F., Cao, J. J., and Jin, Z. D.: Spatial and seasonal variability of water-soluble ions in PM2.5 aerosols in 14 major cities in China, Atmos. Environ., 60, 182–192, https://doi.org/10.1016/j.atmosenv.2012.06.037, 2012.

Choobari, O. A., Zawar-Reza, P., and Sturman, A.: The global distribution of mineral dust and its impacts on the climate system: a review, Atmos. Res., 138, 152–165, https://doi.org/10.1016/j.atmosres.2013.11.007, 2014.

Chung, C. E., Kim, S. W., Lee, M., Yoon, S. C., and Lee, S.: Carbonaceous aerosol AAE inferred from in-situ aerosol measurements at the Gosan ABC super site, and the implications for brown carbon aerosol, Atmos. Chem. Phys., 12, 6173–6184, https://doi.org/10.5194/acp-12-6173-2012, 2012.

339 Dickerson, R. R., Kondragunta, S., Stenchikov, G., Civerolo, K. L., Doddridge, B. G., and
340 Holben, B. N.: The impact of aerosols on solar ultraviolet radiation and photochemical smog,
341 Science, 278, 827–830, https://doi.org/ 10.1126/science.278.5339.827, 1997.

342 EPA: Our nation's air: Status and trends through 2010, U.S. EPA Office of Air Quality
343 Planning and Standards, Research Triangle Park, NC, 2012.

344 Formenti, P., Schütz, L., Balkanski, Y., Desboeufs, K., Ebert, M., Kandler, K., Petzold, A.,
345 Scheuvens, D., Weinbruch, S., and Zhang, D.: Recent progress in understanding physical and
346 chemical properties of African and Asian mineral dust, Atmos. Chem. Phys., 11, 8231–8256,
347 https://doi.org/10.5194/acp-11-8231-2011, 2011.

348 Formenti, P., Caquineau, S., Desboeufs, K., Klaver, A., Chevaillier, S., Journet, E., and Rajot,
349 J. L.: Mapping the physico-chemical properties of mineral dust in western Africa:
350 mineralogical composition, Atmos. Chem. Phys., 14, 10663–10686,
351 https://doi.org/10.5194/acp-14-10663-2014, 2014.

352 Geng, H., Hwang, H., Liu, X., Dong, S., and Ro, C. U.: Investigation of aged aerosols in size-
353 resolved Asian dust storm particles transported from Beijing, China, to Incheon, Korea, using
354 low-Z particle EPMA, Atmos. Chem. Phys., 14, 3307–3323, https://doi.org/10.5194/acp-14-
355 3307-2014, 2014.

356 Griffith, D. R., Martin, W. R., and Eglinton, T. I.: The radiocarbon age of organic carbon in
357 marine surface sediments, Geochim. Cosmochim. Acta, 74, 6788–6800,
358 https://doi.org/10.1016/j.gca.2010.09.001, 2010.

359 Han, Y., Cao, J., Lee, S., Ho, K., and An, Z.: Different characteristics of char and soot in the
360 atmosphere and their ratio as an indicator for source identification in Xi'an, China, Atmos.
361 Chem. Phys., 10, 595–607, https://doi.org/10.5194/acp-10-595-2010, 2010.

362 He, H., Wang, Y., Ma, Q., Ma, J., Chu, B., Ji, D., Tang, G., Liu, C., Zhang, H., and Hao, J.:
363 Mineral dust and NO_x promote the conversion of SO_2 to sulfate in heavy pollution days, Sci.
364 Rep., 4, 4172, https://doi.org/10.1038/srep04172, 2014.

365 Huang, J., Wang, T., Wang, W., Li, Z., and Yan, H.: Climate effects of dust aerosols over
366 East Asian arid and semiarid regions, J. Geophys. Res. Atmos., 119, 19,
367 https://doi.org/10.1002/2014JD021796, 2014.

IPCC, 2007: Climate Change 2007: The Physical Science Basis. Contribution of Working Group I to the Fourth Assessment Report of the Intergovernmental Panel on Climate Change [Solomon, S., D. Qin, M. Manning, Z. Chen, M. Marquis, K. B. Averyt, M. Tignor, and H. L. Miller (eds.)]. Cambridge University Press, Cambridge, United Kingdom and New York, NY, USA, 996 pp.

IPCC, 2013: Climate Change 2013: The Physical Science Basis. Contribution of Working Group I to the Fifth Assessment Report of the Intergovernmental Panel on Climate Change [Stocker, T. F., D. Qin, G.-K. Plattner, M. Tignor, S. K. Allen, J. Boschung, A. Nauels, Y. Xia, V. Bex, and P. M. Midgley (eds.)]. Cambridge University Press, Cambridge, United Kingdom and New York, NY, USA, 1535 pp.

Jin, Q. J, Yang, Z. L., and Wei, J. F.: High sensitivity of Indian summer monsoon to Middle East dust absorptive properties, Sci. Rep., 6, 30690, https://doi.org/10.1038/srep30690, 2016.

Kang, Y., Liu, M., Song, Y., Huang, X., Yao, H., Cai, X., Zhang, H., Kang, L., Liu, X., Yan, X., He, H., Zhang, Q., Shao, M., and Zhu, T.: High-resolution ammonia emissions inventories in China from 1980 to 2012, Atmos. Chem. Phys., 16, 2043–2058, https://doi.org/10.5194/acp-16-2043-2016, 2016.

Kim, J., Lee, J., Lee, H. C., Higurashi, A., Takemura, T., and Song, C. H.: Consistency of the aerosol type classification from satellite remote sensing during the Atmospheric Brown Cloud-East Asia Regional Experiment campaign, J. Geophys. Res. Atmos., 112, D22, https://doi.org/10.1029/2006JD008201, 2007.

Kim, S. B., Yumimoto, K., Uno, I., and Chun, Y.: Dust model intercomparison between ADAM and CFORS/Dust for Asian dust case in 2007 (March 28–April 3), SOLA, 7A, 025–028, https://doi.org/10.2151/sola.7A-007, 2011.

Kunwar, B. and Kawamura, K.: One-year observations of carbonaceous and nitrogenous components and major ions in the aerosols from subtropical Okinawa Island, an outflow region of Asian dusts, Atmos. Chem. Phys., 14, 1819–1836, https://doi.org/10.5194/acp-14-1819-2014, 2014.

Li, J., Wang, Z., Zhuang, G., Luo, G., Sun, Y., and Wang, Q.: Mixing of Asian mineral dust with anthropogenic pollutants over East Asia: a model case study of a super-dust storm in

March 2010, Atmos. Chem. Phys., 12, 7591–7607, https://doi.org/10.5194/acp-12-7591-2012, 2012.

Lim, S., Lee, M., Lee, G., Kim, S., Yoon, S., and Kang, K.: Ionic and carbonaceous compositions of PM_{10}, $PM_{2.5}$ and $PM_{1.0}$ at Gosan ABC Superstation and their ratios as source signature, Atmos. Chem. Phys., 12, 2007–2024, https://doi.org/10.5194/acp-12-2007-2012, 2012.

Lim, S., Lee, M., Kim, S. W., Yoon, S. C., Lee, G., and Lee, Y. J.: Absorption and scattering properties of organic carbon versus sulfate dominant aerosols at Gosan climate observatory in Northeast Asia, Atmos. Chem. Phys., 14, 7781–7793, https://doi.org/10.5194/acp-14-7781-2014, 2014.

Liu, D., Abuduwaili, J., Lei, J., Wu, G., and Gui, D.: Wind erosion of saline playa sediments and its ecological effects in Ebinur Lake, Xinjiang, China, Environ. Earth Sci., 63, 241–250, https://doi.org/10.1007/s12665-010-0690-4, 2011.

McFarlane, N. A., Boer, G., Blanchet, J., and Lazare, M.: The Canadian Climate Centre second-generation general circulation model and its equilibrium climate, J. Clim., 5, 1013–1044, https://doi.org/10.1175/1520-0442(1992)005<1013:TCCCSG>2.0.CO;2, 1992.

Mishra, S. K., Tripathi, S. N., Aggarwal, S. G., and Arola, A.: Effects of particle shape, hematite content and semi-external mixing with carbonaceous components on the optical properties of accumulation mode mineral dust, Atmos. Chem. Phys. Discuss., https://doi.org/10, 31253–31300, 10.5194/acpd-10-31253-2010, 2010.

Nazari, S., Kermani, M., Fazlzadeh, M., Alizadeh-Matboo, S., and Yari, A. R.: The origins and sources of dust particles, their effects on environment and health and control strategies: A review, J. Air Pollut. Health, 1, 137–152, 2016.

Nie, W., Ding, A., Wang, T., Kerminen, V. M., George, C., Xue, L., Wang, W., Zhang, Q., Petäjä, T., Qi, X., Gao, X., Wang, X., Yang, X., Fu, C., and Kulmala, M.: Polluted dust promotes new particle formation and growth, Sci. Rep., 4, 6634, https://doi.org/10.1038/srep06634, 2014.

O'Dowd, C. D., Facchini, M. C., Cavalli, F., Ceburnis, D., Mircea, M., Decesari, S., and Putaud, J. P.: Biogenically driven organic contribution to marine aerosol, Nature, 431, 676–680, https://doi.org/10.1038/nature02959, 2004.

427 Pabortsava, K., Lampitt, R. S., Benson, J., Crowe, C., McLachlan, R., Le Moigne, F. A.,
428 Mark Moore, C., Pebody, C., Provost, P., Rees, A. P., Tilstone, G. H., and Woodward, E.
429 Malcolm S.: Carbon sequestration in the deep Atlantic enhanced by Saharan dust, Nat.
430 Geosci., 10, 189–194, https://doi.org/10.1038/ngeo2899, 2017.

431 Saleh, R., Robinson, E. S., Tkacik, D. S., Ahern, A. T., Liu, S., Aiken, A. C., Sullivan, R. C.,
432 Presto, A. A., Dubey, M. K., Yokelson, R. J., Donahue, N. M., and Robinson, A. L.:
433 Brownness of organics in aerosols from biomass burning linked to their black carbon content,
434 Nature Geosci, advance online publication, 10.1038/ngeo2220,
435 https://doi.org/10.1038/ngeo2220, 2014.

436 Shang, X., Lee, M., Han, J., Kang, E., Kim, S. W., Gustafsson, Ö., Chang, L.: Identification
437 and Chemical Characteristics of Distinctive Chinese Outflow Plumes Associated with
438 Enhanced Submicron Aerosols at the Gosan Climate Observatory, Aerosol Air Qual. Res., 18:
439 330–342, https://doi.org/ 10.4209/aaqr.2017.03.0115, 2018.

440 Shin, S.-K., Müller, D., Lee, C., Lee, K. H., Shin, D., Kim, Y. J., and Noh, Y. M.: Vertical
441 variation of optical properties of mixed Asian dust/pollution plumes according to pathway of
442 air mass transport over East Asia, Atmos. Chem. Phys., 15, 6707–6720,
443 https://doi.org/10.5194/acp-15-6707-2015, 2015.

444 Su, L. and Toon, O. B.: Saharan and Asian dust: similarities and differences determined by
445 CALIPSO, AERONET, and a coupled climate-aerosol microphysical model, Atmos. Chem.
446 Phys., 11, 3263–3280, https://doi.org/10.5194/acp-11-3263-2011, 2011.

447 Tao, J., Gao, J., Zhang, L., Zhang, R., Che, H., Zhang, Z., Lin, Z., Jing, J., Cao, J., and Hsu,
448 S.-C.: $PM_{2.5}$ pollution in a megacity of southwest China: source apportionment and
449 implication, Atmos. Chem. Phys. Discuss., 14, 5147–5196, https://doi.org/10.5194/acpd-14-
450 5147-2014, 2014.

451 Textor, C., Schulz, M., Guibert, S., Kinne, S., Balkanski, Y., Bauer, S., Berntsen, T., Berglen,
452 T., Boucher, O., Chin, M., Dentener, F., Diehl, T., Easter, R., Feichter, H., Fillmore, D., Ghan,
453 S., Ginoux, P., Gong, S., Grini, A., Hendricks, J., Horowitz, L., Huang, P., Isaksen, I., Iversen,
454 I., Kloster, S., Koch, D., Kirkevåg, A., Kristjansson, J. E., Krol, M., Lauer, A., Lamarque, J.
455 F., Liu, X., Montanaro, V., Myhre, G., Penner, J., Pitari, G., Reddy, S., Seland, Ø., Stier, P.,
456 Takemura, T., and Tie, X.: Analysis and quantification of the diversities of aerosol life cycles

within AeroCom, Atmos. Chem. Phys., 6, 1777–1813, https://doi.org/10.5194/acp-6-1777-2006, 2006.

Von Salzen, K., McFarlane, N. A., and Lazare, M.: The role of shallow convection in the water and energy cycles of the atmosphere, Clim. Dynam., 25, 671–688, https://doi.org/10.1007/s00382-005-0051-2, 2005.

Warner, J. X., Dickerson, R. R., Wei, Z., Strow, L. L., Wang, Y., and Liang, Q.: Increased atmospheric ammonia over the world's major agricultural areas detected from space, Geophys. Res. Lett., 44, 2875–2884, https://doi.org/10.1002/2016GL072305, 2017.

World Health Organization, and UNAIDS: Air quality guidelines: global update 2005, World Health Organization, 37–41, 2006.

Yang, M., Howell, S., Zhuang, J., and Huebert, B.: Attribution of aerosol light absorption to black carbon, brown carbon, and dust in China–interpretations of atmospheric measurements during EAST-AIRE, Atmos. Chem. Phys., 9, 2035–2050, https://doi.org/10.5194/acp-9-2035-2009, 2009.

Zender, C. S., Miller, R. L., and Tegen, I.: Quantifying mineral dust mass budgets: Terminology, constraints, and current estimates, EOS Trans., 85, 509–512, https://doi.org/10.1029/2004EO480002, 2004.

Zhang, J.: Coastal saline soil rehabilitation and utilization based on forestry approaches in China, Springer, 11–13, https://doi.org/10.1007/978-3-642-39915-2, 2014.

Zhang, L., Li, Q. B., Gu, Y., Liou, K. N., and Meland, B.: Dust vertical profile impact on global radiative forcing estimation using a coupled chemical-transport–radiative-transfer model, Atmos. Chem. Phys., 13, 7097–7114, https://doi.org/10.5194/acp-13-7097-2013, 2013a.

Zhang, R., Jing, J., Tao, J., Hsu, S.-C., Wang, G., Cao, J., Lee, C. S. L., Zhu, L., Chen, Z., Zhao, Y., and Shen, Z.: Chemical characterization and source apportionment of $PM_{2.5}$ in Beijing: seasonal perspective, Atmos. Chem. Phys., 13, 7053–7074, https://doi.org/10.5194/acp-13-7053-2013, 2013b.

484 Zhang, R. J., Wang, M. X., Zhang, X. Y., and Zhu, G. H.: Analysis on the Chemical and
485 Physical Properties of Particles in a Dust Storm in Spring in Beijing, Powder Technol., 137,
486 77–82, https://doi.org/10.1016/j.powtec.2003.08.056, 2003.

487 Zhang, X. L., Wu, G. J., Zhang, C. L., Xu, T. L., and Zhou, Q. Q.: What's the real role of iron-
488 oxides in the optical properties of dust aerosols?, Atmos. Chem. Phys. Discuss., 15, 5619–
489 5662, https://doi.org/10.5194/acpd-15-5619-2015, 2015.

490 Zhang, X. Y., Zhuang, G. S., Yuan, H., Rahn, K. A., Wang, Z. F., and An, Z. S.: Aerosol
491 particles from dried salt-lakes and saline soils carried on dust storms over Beijing, Terr.
492 Atmos. Ocean. Sci., 20, 619–628, https://doi.org/10.3319/TAO.2008.07.11.03(A), 2009.

493 Zhuang, G., Yi, Z., Duce, R. A., and Brown, P. R.: Link between Iron and Sulfur Suggested
494 by the Detection of Fe (II) in Remote Marine Aerosols, Nature, 355, 537–539,
495 https://doi.org/10.1038/355537a0, 1992.

496

Atmos. Chem. Phys. Discuss., https://doi.org/10.5194/acp-2018-721
Manuscript under review for journal Atmos. Chem. Phys.
Discussion started: 4 September 2018

Atmospheric Chemistry and Physics Discussions

497 Table 1. Mean and mean + σ (standard deviation) concentrations [μg/m^3] of mass and
498 chemical constituents for PM_{10}, $PM_{2.5}$, and PM_1 at GCO during 2007 ~ 2012.

499

	PM_{10}		$PM_{2.5}$		PM_1	
	Mean	Mean+σ	Mean	Mean+σ	Mean	Mean+σ
Mass	30	52	19	32	14	25
Cl^-	0.8	1.7	0.1	0.3	0.1	0.2
NO_3^-	2.1	4.1	1.0	2.2	0.7	1.9
SO_4^{2-}	5.5	9.5	4.4	7.5	4.3	7.5
Na^+	1.2	1.9	0.4	0.7	0.2	0.4
NH_4^+	2.8	4.6	2.4	4.0	2.1	3.6
K^+	0.3	0.5	0.2	0.4	0.2	0.4
Mg^{2+}	0.2	0.3	0.1	0.1	0.02	0.04
Ca^{2+}	0.3	0.7	0.1	0.3	0.1	0.2
OC	4.0	6.6	3.4	5.7	2.6	4.3
OC1	0.1	0.2	0.1	0.2	0.1	0.2
OC2	0.8	1.3	0.8	1.3	0.7	1.1
OC3	1.2	2.0	0.9	1.5	0.7	1.1
OC4	0.9	1.7	0.7	1.3	0.4	0.8
OP	0.9	1.7	0.9	1.6	0.7	1.3
EC	1.5	2.9	1.5	2.7	1.2	2.0
EC1	1.2	2.5	1.1	2.3	0.8	1.5
EC2+EC3	0.3	0.5	0.4	0.6	0.4	0.6

Atmos. Chem. Phys. Discuss., https://doi.org/10.5194/acp-2018-721
Manuscript under review for journal Atmos. Chem. Phys.
Discussion started: 4 September 2018

Atmospheric Chemistry and Physics Discussions

500 Table 2. Intercepts and coefficients for multi-linear regression of PM_{10}, $PM_{2.5}$, and PM_1 mass
501 concentrations using the three principle components (PC1, PC2, and PC3).

502

	PM_{10}	$PM_{2.5}$	PM_1
PC1	4.7	3.1	2.5
PC2	3.7	0.4	−0.7
PC3	4.1	1.9	1.6
Intercept	31.1	19.2	14.8

Atmos. Chem. Phys. Discuss., https://doi.org/10.5194/acp-2018-721
Manuscript under review for journal Atmos. Chem. Phys.
Discussion started: 4 September 2018

Atmospheric Chemistry and Physics Discussions

503 Table 3. The statistical summary for mass concentrations of PM_{10}, $PM_{2.5}$, and PM_1 over entire
504 experiment period [$\mu g/m^3$].

	Median	Mean	S. D. (σ)	Main mode	Mean+σ
PM_{10}	24	30	22	25	52
$PM_{2.5}$	15	19	13	16	32
PM_1	11	14	11	11	25

505

Atmos. Chem. Phys. Discuss., https://doi.org/10.5194/acp-2018-721
Manuscript under review for journal Atmos. Chem. Phys.
Discussion started: 4 September 2018

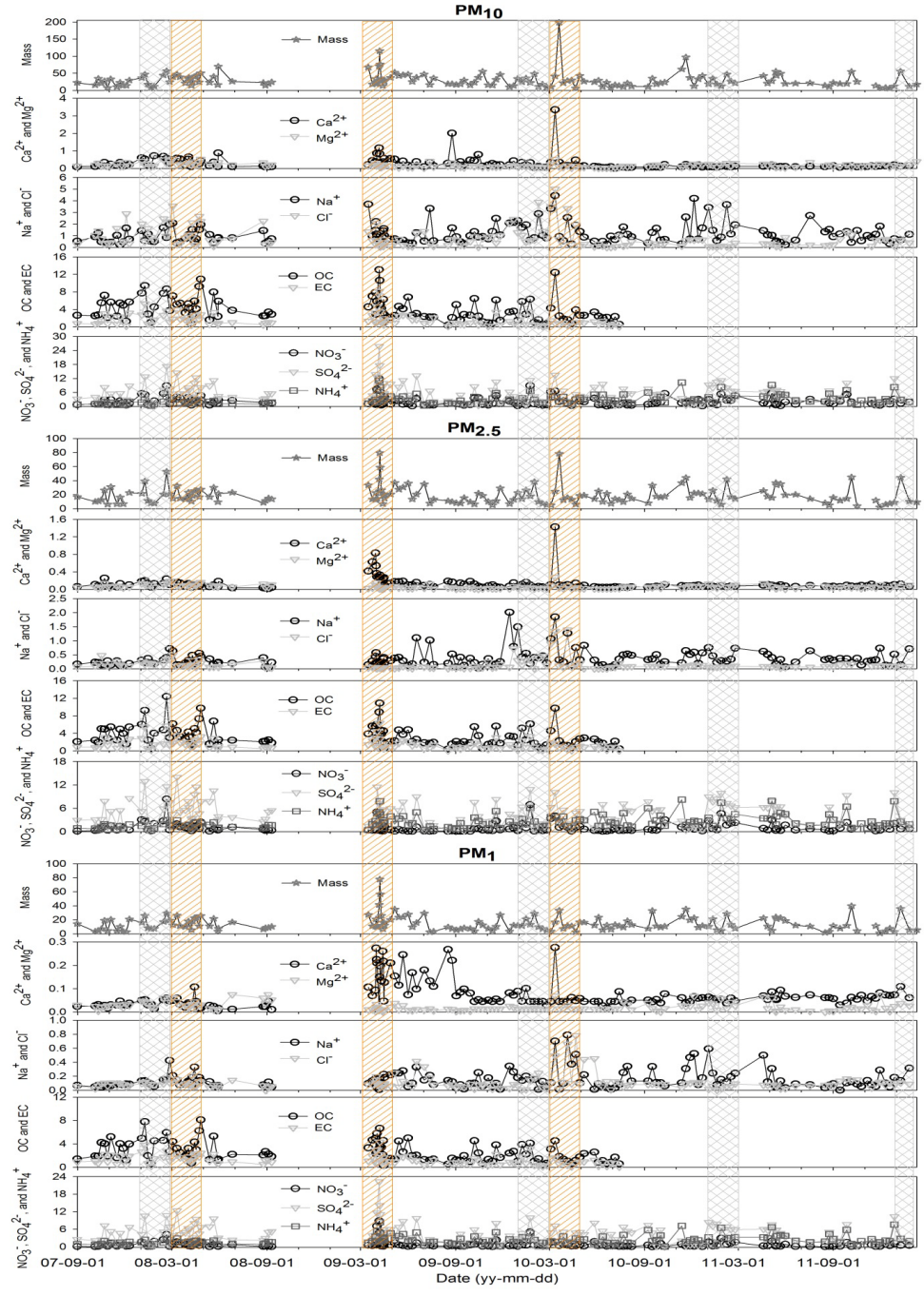

Figure 1. Time-series variations of major constituents of PM_{10}, $PM_{2.5}$, and PM_1 for the entire experiment [$\mu g/m^3$]. Spring and winter periods are shaded in orange and gray.

Atmos. Chem. Phys. Discuss., https://doi.org/10.5194/acp-2018-721
Manuscript under review for journal Atmos. Chem. Phys.
Discussion started: 4 September 2018

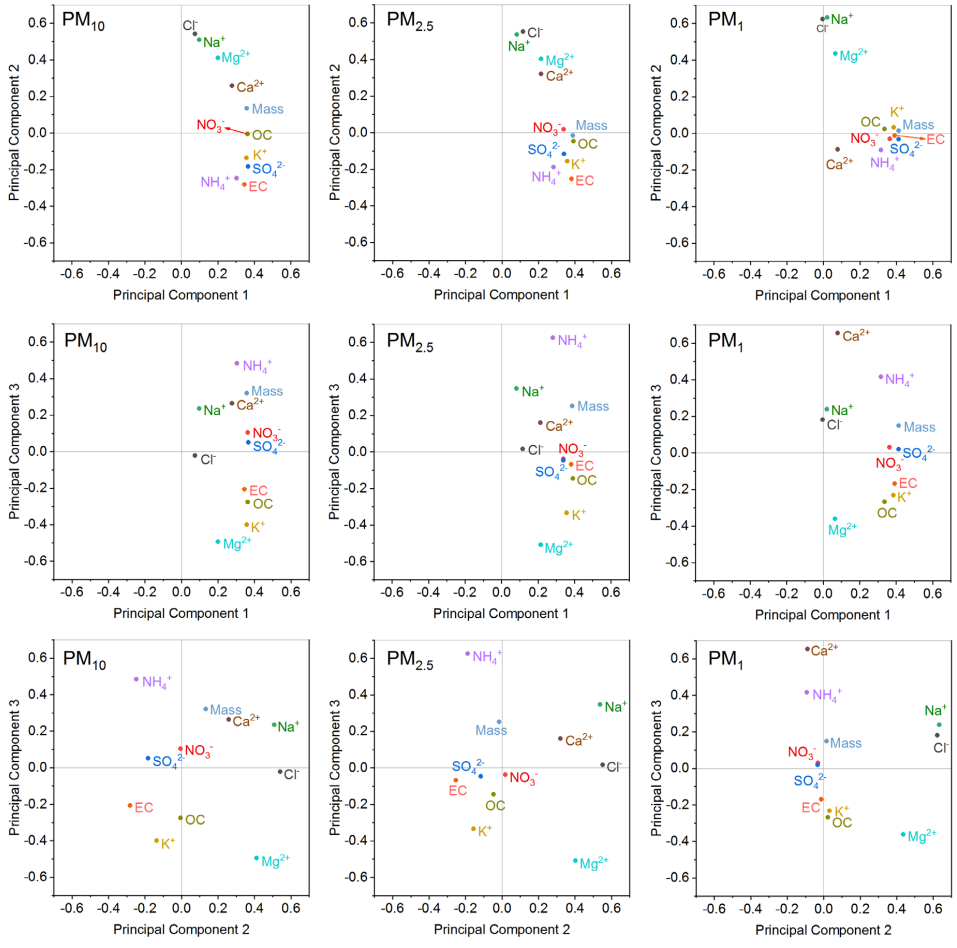

509

510 Figure 2. The results of Principal Component Analysis of all measured species including mass,
511 water-soluble ions, OC, and EC for PM_{10}, $PM_{2.5}$, and PM_1.

Atmos. Chem. Phys. Discuss., https://doi.org/10.5194/acp-2018-721
Manuscript under review for journal Atmos. Chem. Phys.
Discussion started: 4 September 2018

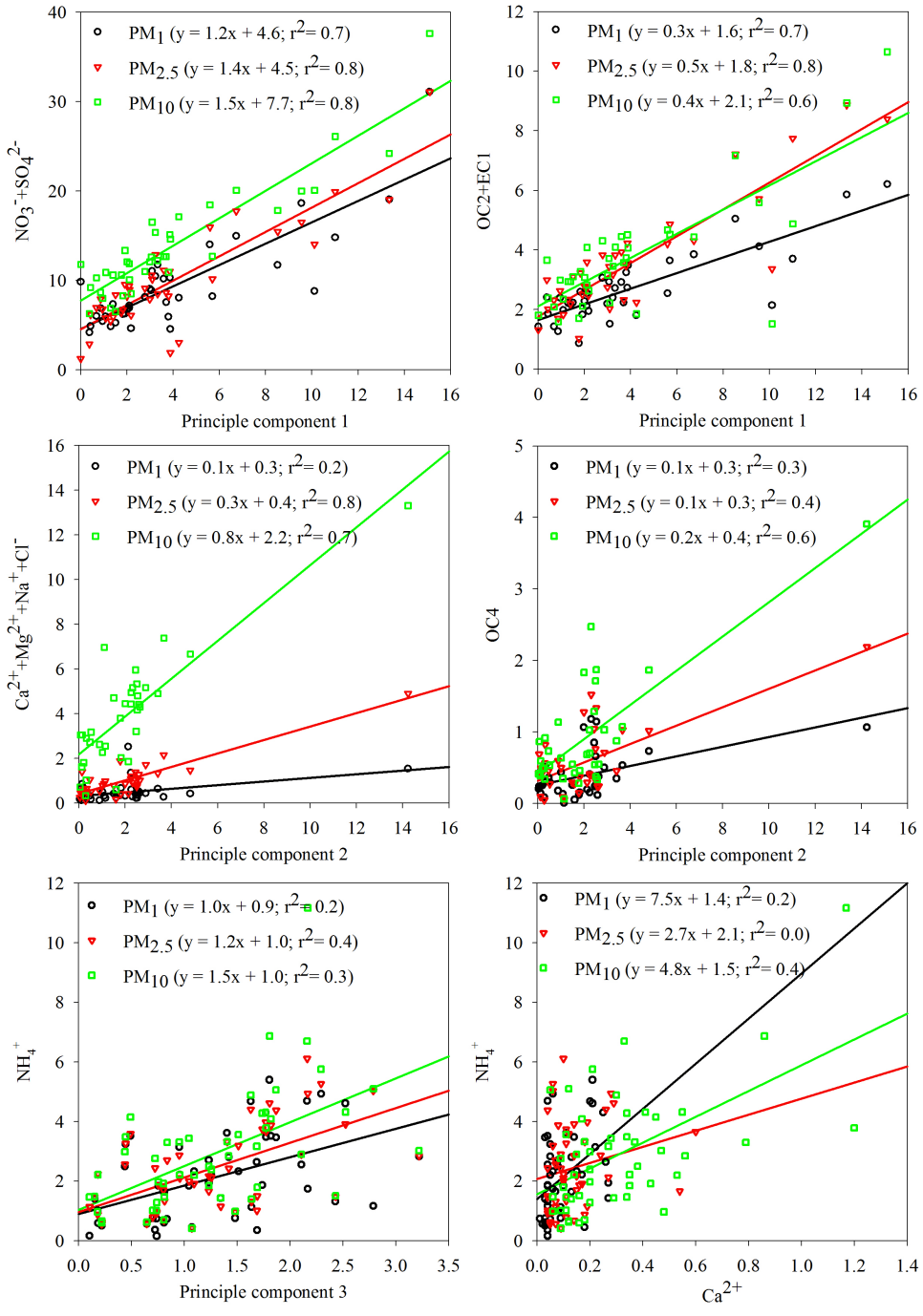

Figure 3. Correlations between the three principle component loadings and major species concentrations [μg/m^3] for PM_{10}, $PM_{2.5}$, and PM_1.

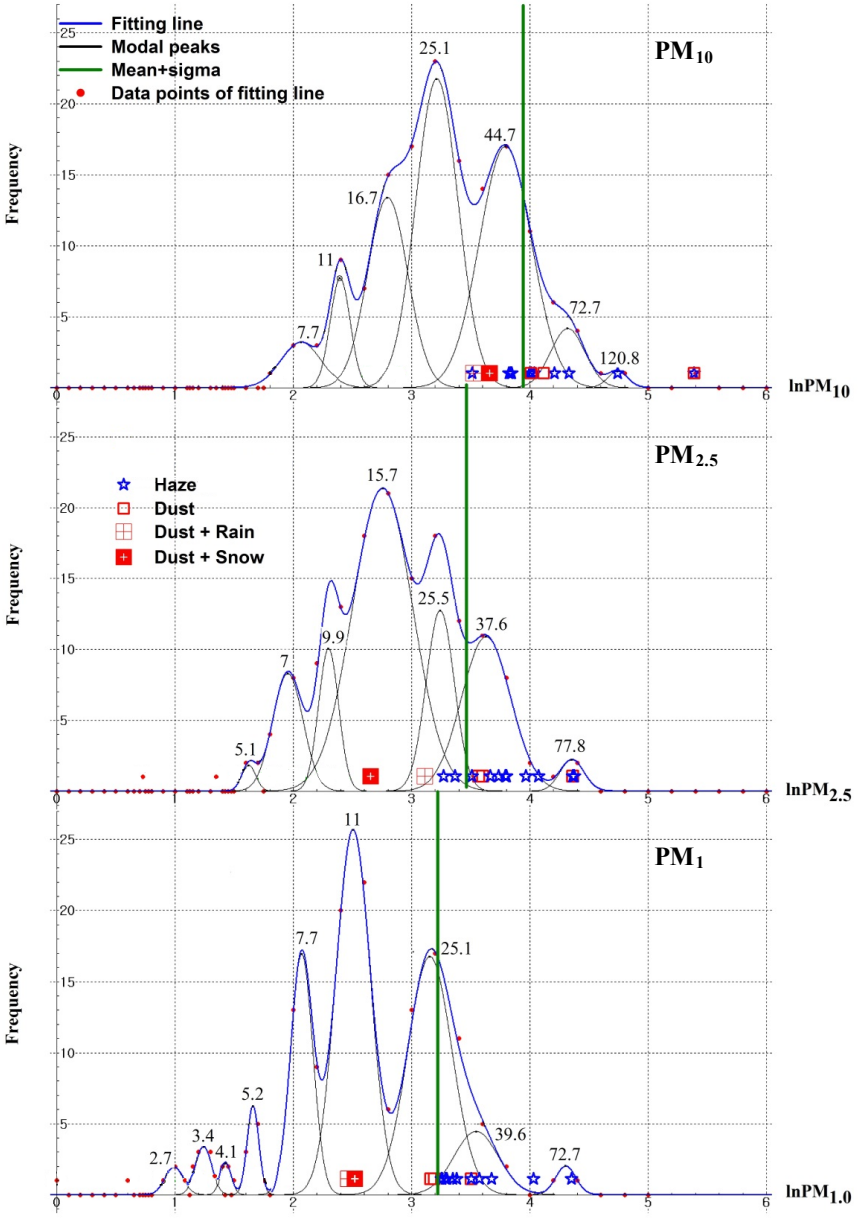

Figure 4. Frequency distributions of PM_{10}, $PM_{2.5}$ and PM_1 mass concentrations for all measurements. Mass concentrations are given as ln values in x-axis. The green lines stand for mean+σ. The individual samples collected during dust or haze events are marked as different symbols along the x-axis.